A DOUBLE SOFTLITHOGRAPHY METHOD FOR PROCESSING OF NOA63 MICRONEEDLES ARRAYS

Florina Silvia ILIESCU[1]*, Stana PAUNICA[2], Danilo VRTAČNIK[3], Andreea Rodica BOBEI (STERIAN)[4]

The present paper proposed a simple method using a double softlithography process for the fabrication of microneedles (MNs) arrays. A biocompatible UV curable polymer, Norland Optic Adhesive-NOA63 was selected to fabricate the solid hydrophilic microneedles. The geometry and the penetration capabilities of the newly fabricated microneedles were evaluated by optical imaging and microCT. The results evidenced that the length of the newly created MNs was acceptable for the intended purpose. The insertion tests evaluated the sharpness and robustness of the NOA63 MNs: the MNs were able to pierce the skin samples. These tests also highlighted the influence of the insertion force upon the penetration capability. The NOA63 MNs proved compliant with the general requirements. Moreover, they presented the advantage of a low-cost fabrication process. Therefore, the newly created MNs are promising alternative devices able to disrupt effectively the cutaneous barrier.

Keywords: transdermal drug delivery, microneedles, biocompatible polymer, microCT, softlithography

1. Introduction

Medicine and pharmacy have a common goal: to alleviate and/or cure patients' conditions with the help of methods which deliver therapeutic agents to the specific target, at the right moment, at the right concentration level, in a safe and reproducible manner. A wide range of therapeutic modalities and formulations permitted individualized therapeutic schemes. Alternatives to the oral route, the preferred method developed in order to address the impossibility of adequate administration and the related low bioavailability of peptide or protein drugs [1]. Out of the valid modalities for drug administration currently used in the medical field, the transdermal drug delivery (TDD) [2] advanced to improve drug transport across the skin with the help of chemical enhancers [3], iontophoresis

[1] PhD; Senior Lecturer, School of Applied Science, Republic Polytechnic, Singapore, e-mail: florina_iliescu@rp.edu.sg
[2] PhD; Assoc. Prof. University of Medicine and Pharmacy, Bucharest, Romania
[3] PhD; Laboratory of Microsensor Structures and Electronics, Faculty of Electrical Engineering, University of Ljubljana, Slovenia, e-mail: danilo.vrtacnik@fe.uni-lj.si
[4] PhD; Lecturer, Physics Department, University POLITEHNICA of Bucharest, Romania

[4], electroporation [5], sonophoresis [6], mechanical enhancers (microneedles arrays) [7-9], or their combinations [10, 11].

The advances of the emerging microfabrication techniques [12-17] introduced novel and trustable drug delivery systems such as microfabricated nanoparticles, [18-21] microfluidic chips [22, 23], and microneedles-MNs [24-26]. All expressed superior structural, mechanical, electronic properties [12, 27] as well as cost-effectiveness for mass production [28]. The significant feature of MEMS products [29] and of microneedles in particular, is that they can be specifically designed for minimal invasiveness and for programmed drug release.

The first MNs were made of silicon using microfabrication techniques [30, 31], and the procedure developed further using stainless steel [32], palladium [33], titanium [34], nickel [35], glass, ceramics, zeolite [36]. However, the technological advantages such as the well-controlled microfabrication processes methods, the precise and controllable 3-dimensional structures [37], and the affordable mass production were outshined by the major biological side effects caused by the brittleness and biohazardous sharpness with risk of local inflammation or blood borne diseases [38]. Since the only biocompatible metal MNs were of porous silicon [39, 40], the implementation of new biomaterials became imperious. Various polymers including polyvinyl acetate [41], poly-etherimide [42], polycarbonate [43], poly-ethylene glycol [44], and poly-lactide-co-glycolide [45] have been used. Sugars and sugar derivatives such as dextrose [46], maltose [47], or galactose [48] have also been considered. These materials are biocompatible, cost-effective, generate no biohazardous waste and the fabrication involved micromoulding techniques [45]. However, limitations remained: high temperature processing, quick dissolution of the MNs, resulting in less control over drug release, instability under humid conditions, UV crosslinking requirements, and drug materials/process incompatibility that can impact the potency of the compounds to be delivered.

The present work discusses the use of one biocompatible polymer, NOA63 and the soft lithography in fabrication of MNs in accordance with the clinical purpose. The processed MNs were characterized using optical and X-ray imaging modalities, and their penetration capability in pigskin was assessed.

2. Materials and methods

2.1. Polymers

Two polymers were employed: PDMS (Sylgard® 184 - Polydimethyl siloxane, Down Corning, USA) and Norland Optic Adhesive-NOA63 (Norland Products, NJ, USA). NOA63 is an UV curable, clear liquid adhesive with density >1. None of the ingredients of this UV Curing Adhesive (Mercapto-ester, Triallyl Isocyanurate) are listed as carcinogens in NTP, IARC, OSHA, RoHS, REACH or

any state's list of chemicals known to cause reproductive toxicity. Therefore, NOA63 is a biocompatible polymer.

2.2 Skin Tissue Processing for Imaging

Full thickness porcine cadaver skin with adipose layers was used. Skin tissues were kept frozen at –20°C until used. The skin tissue was prepared by removing the fat layer (using a surgical blade) and thawed completely (for 30 min) to room temperature. The skin sample was flattened onto a wooden block with 10 to 12 layers of Kimwipes underneath. The final sample was 1-1.5mm thick.

2.3 Scanning electron microscopy

(SEMs) images were taken using a JEOL SEM (JSM-6701F Field Emission Scanning Electron Microscope). Samples were prepared by coating with a thin layer (a few nanometers) of gold and mounted onto sample holders (JFC-1600 Auto Fine Coater). Images were retrieved at various magnifications.

2.4 MicroCT

MicroXCT400 (XRadia) was used to image the MNs during the penetration test into the pigskin. MNs were applied onto the skin sample and mounted onto the sample holder. MN patches were applied on the flat skin surface for 1 min using weights equivalent to 4.5N, 10N, 13N and 22N. Controls consisted of skin not treated with MNs. The imaging procedure used exposure parameters for soft tissues.

2.5. Optical Imaging

For the insertion test, the skin sample was covered with Methylene Blue (tissue dye used in histology) and MNs were applied. The application of the MNs onto the skin was similar to the X-ray imaging procedure. The number of the entry points was observed after the MNs and the excess of dye (ethanol 70%) were removed. Bright field images of the tissue samples were taken using a dissection microscope (Zeiss Stemi DV4). A digital camera (Canon) was used to take the digital pictures of the moulds, MNs and of the entry points MNs produced on the skin samples.

3. Microneedles design and fabrication

3.1 Fabrication of the Si mould with array of microneedles

The Si microneedles array used as mould was fabricated on a 4” silicon wafer, 1mm-thick, double polished, with <100> crystallographic orientation using microfabrication techniques (Fig. 1a). A 2μm-thick low stress SiN_x layer was

deposited on the surface of the Si wafer using a PECVD reactor [49, 50]. A second deposition -Al- (2µm-thick) was processed using an e-beam evaporator (Fig. 1b). A 6µm-thick photoresist mask (AZ4620- Clairant) was developed on Al surface for patterning of Al and SiN_x layers (Fig 1c). The etching of Al layer was performed with commercially available Al wet etching solution while for SiN_x layer a plasma process in a RIE reactor using CHF_3/O_2 chemistry was performed (Fig 1d). A 500µm deep isotropic etching was performed through the above mentioned created mask using a deep RIE system and SF_6/O_2 process (Fig. 1e). The process continued till the mask was self-removed. The isotropic process and a Teflon coating in plasma were performed for an easily demoulding process (Fig. 1f).

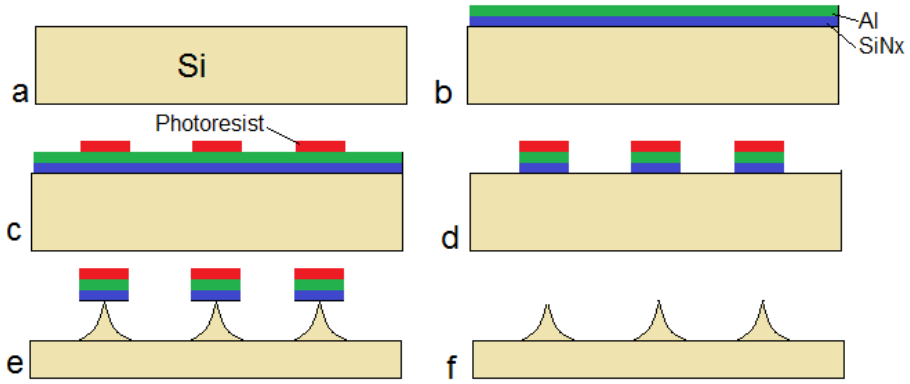

Fig. 1. Main steps of the fabrication process of the Si mould: a) Si wafer; b) deposition of the SiNx and Al; c) photoresist mask; d) etching of the Al and SiNx; e) isotropic etching of the Si; f) Teflon coating

3.2. The double softlithography process

The moulding process described in Fig. 2. is a double softlithography-based process. It had Silicon (Si) MNs as first hard master (Fig. 2a). Each plate consisted of 60 MN arrays of $1cm^2$ and 1mm thickness each. Each array comprised a matrix of 9x9 Si MNs. The average length of Si MN was 500µm. The steps comprised soft lithography which helped form the necessary patterns by polymerization templated by the hard masters. First, PDMS was utilized as a molding material to produce the second master. The embedding elastomer was mixed according to supplier specifications and degassed in vacuum for 45min. The mould patterns of Si MNs were transferred onto PDMS by casting the Sylgard® 184 (silicon elastomeric base and curing agent mixed in 10:1 ratio) onto the Si MN array and allowed to cure and dry to solidify at 125°C for 30min. Fig. 2b depicts the Si MNs plate covered by PDMS after curing. Fig. 2c shows the final PDMS MNs replica. Attention was paid to remove the gas bubbles existing in the master mix, prior the curing. The next step used NOA63 and the PDMS

MNs replica. The MNs pattern was transferred into NOA63 by casting the elastomer. It was poured onto PDMS template and degassed in vacuum. After the PDMS mould was filled with NOA63 gel the excess of NOA63 gel was removed. (Fig. 2c) This step was followed by polymerization via UV exposure (Polylux 500 UV Curing oven) which allowed NOA63 to cure and dry to solidify (Fig. 2d).

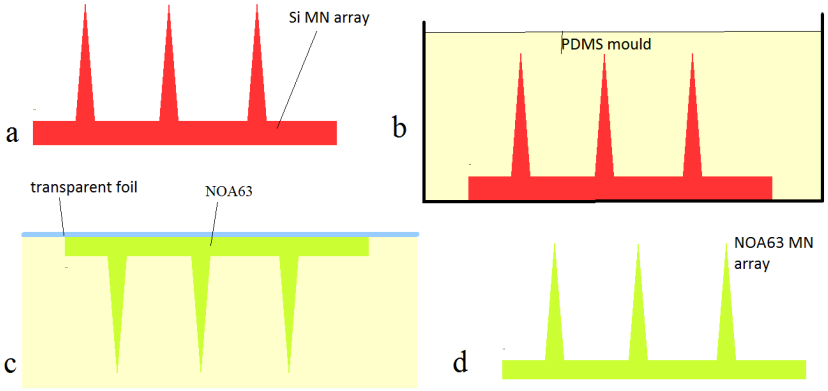

Fig. 2. The process of fabrication of polymer MNs: a) Si MNs fabricated using MEMS technology; b) processing PDMS replica; c) deposition of NOA63 on the PDMS mold; d) NOA63 MNs array after UV curing using PDMS

The NOA63 replica was then detached from its PDMS master. Images with the main step of the fabrication are presented in Fig. 3.

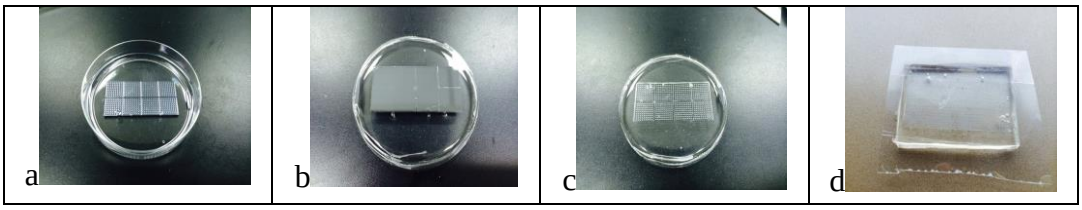

Fig. 3. The steps taken to fabricate the solid, hydrophilic biocompatible MNs: a. The Si MNs plate; b. The Si MNs master covered with PDMS; c. The PDMS MNs replica; d. The PDMS replica covered with NOA63

Both methods relied on the physical contact of the stamp/probe with the substrate. Physical contact is the key mediator of pattern transfer and is, in principle, limited only by van der Waals contact and the inherent atomic and molecular granularity of matter. Therefore, desiccation was one essential step in the process.

4. Results and discussions

Microneedles design and fabrication

Soft lithography has had recognized practical advantages in the field of biology as one alternative to photolithography, and an unconventional approach to nanofabrication and pattern transfer. [52]. The use of soft lithography principles allowed the micromoulding of Si MNs into NOA63 biocompatible, solid, hydrophilic MNs. The process comprised two steps, which proved rapid, easily controllable and consistent. Both polymers proved capable of polymeric (usually elastomeric) stamps bearing relief features to transfer micropatterns. Moreover, it didn't require special training, was easily repeatable, safe and cost-effective. Such characteristics matched the general description of microtechnology well known for its mass production potential. Fig. 4. macroscopically describes the NOA63 MNs. NOA63 allowed the production of thin, much flexible than Si MNs, and resistant MNs arrays.

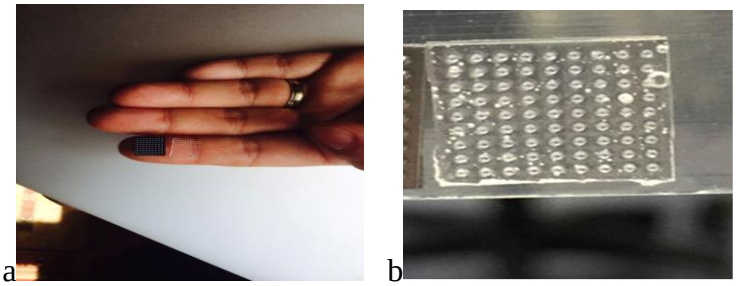

Fig. 4. a. The compared Si and NOA63 MNs; b. A matrix of NOA63 MNs

Imaging

Since 1979 when the concept of micron scale arrays able to transiently breach the stratum corneum emerged, the fabrication of MNs evolved from the sharp tips 150µm model of Henry *et al* [30] to a multitude of geometries to address the specific applications. The imaging procedures permitted the assessment of the NAO63 MNs microscopic structures and penetration functions. SEM imaging evidenced the geometry of the newly fabricated MNs. Fig. 5 presents various aspects of the geometry of the newly created NOA63 MNs compared with their Si counterparts.

Since the length of MNs accepted for successful painless drug administration varies from 50µm to 1000µm, [51] the length of the new NOA63 MNs (average 320 µm) can also be acceptable for the intended purpose. This evaluation concluded the ability of the method to deliver NOA63 replica geometrically similar to the Si masters. Compared with metal which is highly malleable and relatively easy to be shaped into sharp, narrow and long MNs, polymers are less tractable. The geometry obtained proved the potential of NOA63 in this area due to the possibility to obtain stability, length, and sharpness.

Moreover, the nontoxic propriety of NOA63 is one essential feature to support the NOA63 MNs' potential as no biological hazards in TDD. The microCT imaging tests visualized the capacity of NOA63 MN to penetrate the superficial layer of skin (stratum corneum) at various application forces (4.5N, 10N, 13N, 22N).

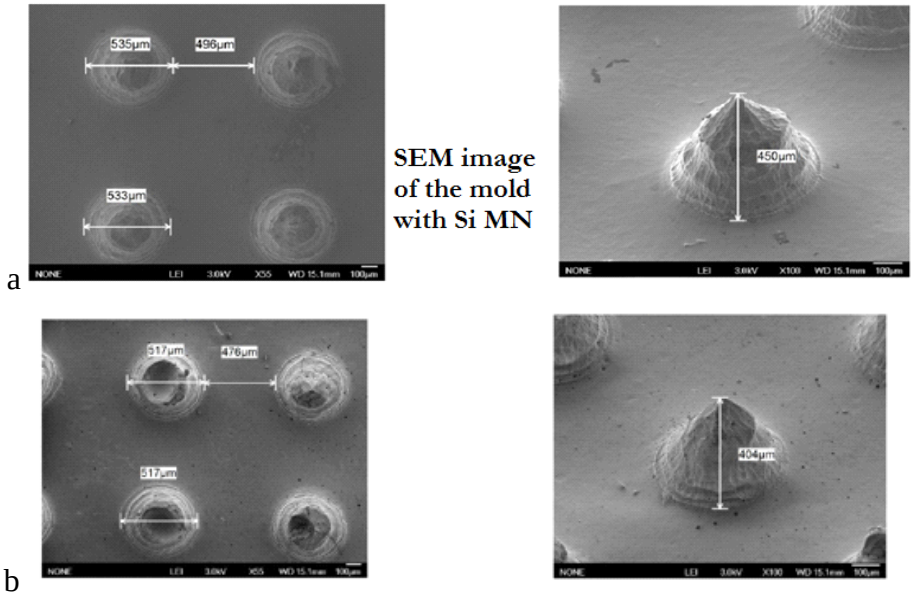

Fig. 5. The SEM images of MNs to evidence the geometry at 20x and 100x magnification: a. the Si MNs geometry; b. the NOA63 MNs geometry

The MNs-skin interface was assessed for Si and NOA63 MNs. At that location, due to the various densities of the materials exposed to X-ray, X-ray photons were absorbed differently. The area in the microCT image which evidenced less contrast (lighter grey) due to low density material and lower absorption of X-ray photons corresponded to the air gaps at the MNs - skin, and the MNs - plastic holder interfaces. The area with increased contrast (intense grey) due to higher density material represented the MNs inserted into the skin.

The superposition of the MNs' and tissues' densities explained the increased contrast. To further enhance the contrast at the MNs – skin border we applied Iodine as contrast agent. The air gap at the interface between the skin and the MN array was observed to decrease with the increase of the insertion force (Fig. 6). The insertion of MNs proved to be better at higher insertion force applied. The results of insertion test showed the densities of the micropores created by the NOA63 MNs (Fig. 7).

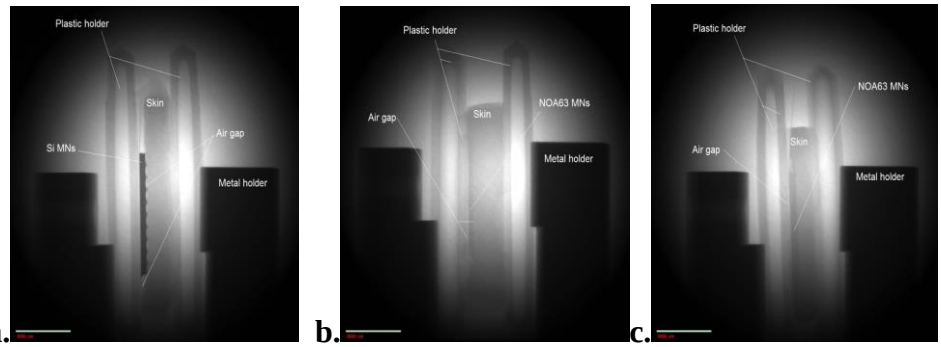

a. **b.** **c.**

Fig. 6. The results of the micro-CT imaging test show how MNs pierced the superficial layers of the skin samples: a. Si MNs at 4.5N applied force with a visible air gap between the MNs array and the skin surface and b. NOA63 MNs at 4.5N applied force with a visible air gap between the MNs array and the skin surface; c. NOA63 MNs at 22N applied force with a better contact surface between the MNs and the skin

It was observed that the area treated with MNs had well defined margins and also rows of micropores with a regular distribution. This pattern corresponded to the MNs array and showed the MNs capability of penetrating the skin surface. The patterns produced by MNs applied onto the skin added to the natural aspect of the skin. However, the area adjacent to the MNs contact area was not treated with MNs, and presented an irregular distribution of the micropores corresponding to the natural aspect of the skin (Fig. 7). Such results evidenced the NOA63 sharpness and robustness. The counting of the entry points visible at the surface of the skin sample showed how the insertion of NOA63 MNs took place at various insertion forces applied (4.5N force corresponds to a light thumb pressure, 10N to a medium thumb pressure, 13N to a normal thumb pressure, 22N to high thumb pressure). Fig. 8 depicts the correlation between the insertion forces applied and the penetration capacity of the MNs (the density of the micropores created).

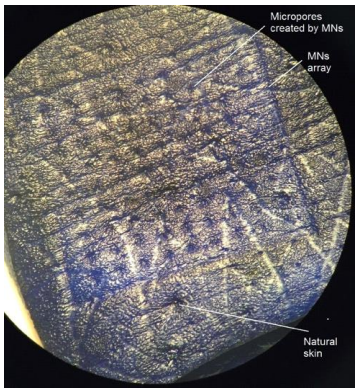

Fig. 7. The image of entry points created by the MNs into the skin colored with Methylene Blue

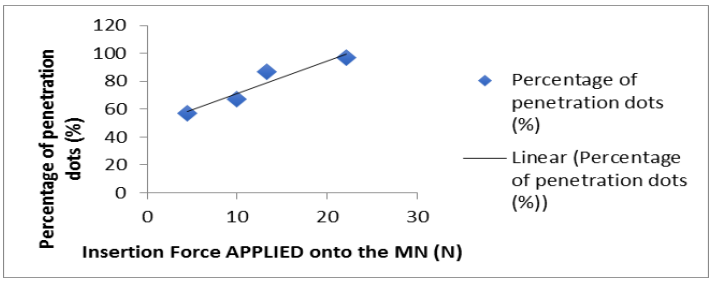

Fig. 8. The percentage of entry points correlated with the insertion force applied

The positive correlation (r= 0.94) indicated the increase in density of the entry points with the insertion force applied. 90% was achieved with 13N force and 100% insertion at higher force.

4. Conclusions

The current work addressed the geometry and the insertion capability of newly created biocompatible solid NOA63 MNs.

The results indicated the potential of NOA63 MNs from both perspectives. First, the length of the new NOA63 MNs (average 320 µm) can be acceptable for the intended purpose. Moreover, the imaging and insertion tests indicated the ability of the NOA63 MNs to pierce skin samples. The results highlighted the influence the insertion force has on the penetration capability, and indicated the positive correlation between the piercing capability of the MNs and the force applied for their insertion into the skin samples used. The normal thumb pressure may facilitate the successful insertion of the MNs. Consequently, the NOA63 MNs have the advantage of being compliant with the general requirements and produced with a low-cost fabrication process. This will further support the MNs as recognized and promising alternative to introduce medicine into the human body.

R E F E R E N C E S

[1] *A. Hoffman*, In Controlled Drug Delivery: Challenges and Strategies; Park, K., Ed. American Chemical Society: Washington, DC; 1997.

[2] *M.R. Prausnitz, R. Langer*, "Transdermal drug delivery", Nature Biotechnology, **vol. 26**, no. 11, 2008, pp. 1261-1268.

[3] *J.J. Escobar-Chávez, I.M. Rodríguez Cruz, C.L. Domínguez Delgado, L. Gallelli*, "Chemical and Physical enhancers for transdermal drug delivery", Pharmacology Rijeka: InTech. pp. 397-433, 2012.

[4] *R.H. Guy, Y.N. Kalia, M.B. Delgado-Charro, V. Merino, A. López, D. Marro*, "Iontophoresis: electrorepulsion and electroosmosis", Journal of Controlled Release, **vol. 64**, no. 1, 2006, pp. 129-132.

[5] *A.K. Banga, S. Bose, T.K. Ghosh*, "Iontophoresis and electroporation: comparisons and contrasts". International Journal of Pharmaceutics, **vol. 179,** no. 1, 1999, pp. 1-19.

[6] *D. Park, H. Park, J. Seo, S. Lee*, "Sonophoresis in transdermal drug deliverys", Ultrasonics, **vol. 54**, no. 1, 2014, pp. 56-65.

[7] *M.W. Ashaf, S. Tayyaba, N. Afzulpurkr*, "Tapered tip hollow silicon microneedles for transdermal drug delivery. 2nd International Conference on Mechanical and Electronics Engineering (ICMEE); 2010: IEEE.

[8] *H. Kathuria, J.S. Kochhar, M.H.M. Fong, M. Hashimoto, C. Iliescu, H. Yu, L. Kang*, "Polymeric Microneedle Array Fabrication by Photolithography", JoVE (Journal of Visualized Experiments), **vol. 105**, 2015, art. no:e52914-e.

[9] *H. Li, Y.S.J. Low, H.P. Chong, M.T. Zin, C-Y Lee, B. Li, et al*, "Microneedle-mediated delivery of copper peptide through skin", Pharmaceutical Research, **vol. 32**, no. 8, 2015, pp. 2678-2689.

[10] *B. Chen, J. Wei, C. Iliescu*, "Sonophoretic enhanced microneedles array (SEMA)—Improving the efficiency of transdermal drug delivery", Sensors and Actuators B: Chemical, **vol. 145**, issue 1, 2010, pp. 54-60.

[11] *M. Petchsangsai, T. Rojanarata, P. Opanasopit, T. Ngawhirunpat*, "The combination of microneedles with electroporation and sonophoresis to enhance hydrophilic macromolecule skin penetration", Biological and Pharmaceutical Bulletin, **vol. 37**, issue 8, 2014, pp. 1373-1382.

[12] *I. Cima, C.W. Yee, F.S. Iliescu, W.M. Phyo, K.H. Lim, C. Iliescu, M.H. Tan*, "Label-free isolation of circulating tumor cells in microfluidic devices: Current research and perspectives", Biomicrofluidics, **vol. 7**, issue 1, 2013, art. no: 011810.

[13] *F.S. Iliescu, A.P. Sterian, E. Barbarini, M. Avram, C. Iliescu*, "Continuous separation of white blood cell from blood in a microfluidic device", UPB Scientific Bulletin, Series A: Applied Mathematics and Physics. 2009;71(4), pp. 21-30.

[14] *B. Lazar, A. Sterian, S. Pusca, V. Paun, C. Toma, C. Morarescu*, "Simulating delayed pulses in organic materials", In: Gavrilova M, Gervasi O, Kumar V, Tan CJK, Taniar D, Lagana A, et al., editors. Computational Science and Its Applications - Iccsa 2006, Pt 1. Lecture Notes in Computer Science. 3980. Berlin: Springer-Verlag Berlin; 2006. pp. 779-84.

[15] *M. Ni, W.H. Tong, D. Choudhury, N.A.A. Rahim, C. Iliescu, H. Yu*, "Cell culture on MEMS platforms: A review" International Journal of Molecular Sciences, **vol. 10**, issue 12, 2009, pp. 5411-5441.

[16] *F. Yu, F.S. Iliescu, C. Iliescu*, "A Comprehensive Review on Perfusion Cell Culture Systems". *Informacije MIDEM*, **vol. 46**, no. 4, 2016, pp. 163-175.

[17] *C. Moldovan, R. Iosub, C. Codreanu, B. Firtat, D. Necula, C. Brasoveanu, et al.*, "Miniaturized Integrated Platform for Electrical and Optical Monitoring of Cell Cultures", Sensors, **vol. 12**, issue 8, 2012, pp. 11372-11390.

[18] *C. Iliescu, G. Tresset*, "Microfluidics-Driven Strategy for Size-Controlled DNA Compaction by Slow Diffusion through Water Stream", Chemistry of Materials, **vol. 27**, issue 24, 2015, pp. 8193-8197.

[19] *C. Iliescu, C. Mărculescu, S. Venkataraman, B. Languille, H. Yu, G. Tresset*, "On-chip controlled surfactant–DNA coil–globule transition by rapid solvent exchange using hydrodynamic flow focusing", Langmuir, **vol. 30**, issue 44, 2014, pp. 13125-13136.

[20] *G. Tresset, C. Marculescu, A. Salonen, M. Ni, C. Iliescu*, "Fine control over the size of surfactant–polyelectrolyte nanoparticles by hydrodynamic flow focusing", Analytical Chemistry, **vol. 85**, issue 12, 2013, pp. 5850-5856.

[21] *G. Tresset, C. Iliescu*, "Microfluidics-Directed Self-Assembly of DNA-Based Nanoparticles" Informacije MIDEM, **vol. 46**, no.4, 2016, pp. 183-189.

[22] *F.S. Iliescu, C. Iliescu*, "Circulating Tumor Cells Isolation Using On-Chip Dielectrophoretic Platforms", Annals of the Academy of Romanian Scientists Series on Science and Technology of Information, **vol. 9**, no. 2, 2016, pp. 27-42.
[23] *D.P. Poenar, C. Iliescu, J. Boulaire, H. Yu*, "Label-free virus identification and characterization using electrochemical impedance spectroscopy", Electrophoresis, **vol. 35**, issue 2-3, 2014, pp. 433-40.
[24] *D. Resnik, M. Možek, B. Pečar, T. Dolžan, A. Janež, V. Urbančič, et al.*, "Characterization of skin penetration efficacy by Au-coated Si microneedle array electrode", Sensors and Actuators A: Physical, **vol. 232**, 2015, pp. 299-309.
[25] *F.S. Iliescu, A.P. Sterian, M. Petrescu*, "A parallel between transdermal drug delivery and microtechnology" UPB Scientific Bulletin, Series A: Applied Mathematics and Physics, **vol. 75,** no. 3, 2013, pp. 227-236.
[26] *J. Ji, F.E.H. Tay, J. Miao, C. Iliescu*, "Microfabricated silicon microneedle array for transdermal drug delivery", Journal of Physics: Conference Series; **vol. 34**, May 2006, pp. 1127-1131.
[27] *T. Das, S. Chakraborty*, "Perspective: Flicking with flow: Can microfluidics revolutionize the cancer research?", Biomicrofluidics, **vol. 7**, issue 1, 2013, art. no"011811.
[28] *D. Choudhury, D. van Noort, C. Iliescu, B. Zheng, K-L Poon, S. Korzh, et al*., "Fish and Chips: a microfluidic perfusion platform for monitoring zebrafish development", Lab on a Chip, **vol. 12**, issue 5, 2012, pp. 892-900.
[29] *A.C. Richards Grayson, R. Scheidt Shawgo, Y. Li, M.J. Cima*, "Electronic MEMS for triggered delivery", Advanced Drug Delivery Reviews, vol. 56, issue 2, 2004, pp. 173-184.
[30] *S. Henry, D. McAllister, M. Allen, M. Prausnitz*, "Microfabricated microneedles: A novel approach to transdermal drug delivery", Journal of Pharmaceutical Sciences, **vol. 88**, issue 9, 1999, pp. 948.
[31] *R.F. Donnelly, D.I. Morrow, P.A. McCarron, A. David Woolfson, A. Morrissey, P. Juzenas, et al*., "Microneedle arrays permit enhanced intradermal delivery of a preformed photosensitizer", Photochemistry and Photobiology, vol. 85, issue 1, 2009, pp. 195-204.
[32] *H.S. Gill, M.R. Prausnitz*, "Coated microneedles for transdermal delivery", Journal of Controlled Release, vol. 117, issue 2, 2007, pp. 227-237.
[33] *S. Chandrasekaran, J.D. Brazzle, A.B. Frazier*, "Surface micromachined metallic microneedles", Journal of Microelectromechanical Systems, **vol. 12**, issue 3, 2003, pp. 281-288.
[34] *E. Parker, M. Rao, K. Turner, C. Meinhart, N. MacDonald*, "Bulk micromachined titanium microneedles" Journal of Microelectromechanical Systems, **vol. 16**, issue 2, 2007, pp. 289-295.
[35] *N. Roxhed, B. Samel, L. Nordquist, P. Griss, G. Stemme*, "Painless drug delivery through microneedle-based transdermal patches featuring active infusion", Biomedical Engineering, IEEE Transactions on, **vol. 55**, no. 3, 2008, pp. 1063-1071.
[36] *S. Gittard, R. Narayan, C. Jin, A. Ovsianikov, B. Chichkov, N. Monteiro-Riviere, et al*., "Pulsed laser deposition of antimicrobial silver coating on Ormocer® microneedles", Biofabrication, **vol. 1**, no. 4, 2009, art. no: 041001.
[37] *L. Wei-Ze, H. Mei-Rong, Z. Jian-Ping, Z. Yong-Qiang, H. Bao-Hua, L. Ting, et al*., "Super-short solid silicon microneedles for transdermal drug delivery applications", International Journal of Pharmaceutics, **vol. 389**, issue 1-2, 2010, pp. 122-129.
[38] *S. Bystrova, R. Luttge*, "Micromolding for ceramic microneedle arrays", Microelectronic Engineering, **vol. 88**, issue 8, 2011, pp. 1681-1684.
[39] *B. Chen, J. Wei, F.E. Tay, Y.T. Wong, C. Iliescu*, "Silicon microneedle array with biodegradable tips for transdermal drug delivery", Microsystem Technologies **vol. 14**, issue 7, 2008, pp.1015-1019.

[40] *J. Ji, F.E.H. Tay, J. Miao, C. Iliescu*, "Microfabricated microneedle with porous tip for drug delivery", Journal of Micromechanics and Microengineering, **vol. 16**, no. 5, 2006, pp. 958-964.

[41] *R.F. Donnelly, R. Majithiya, T.R.R. Singh, D.I. Morrow, M.J. Garland, Y.K. Demir*, "Design, optimization and characterisation of polymeric microneedle arrays prepared by a novel laser-based micromoulding technique", Pharmaceutical Research, **vol. 28**, issue 1, 2011, pp. 41-57.

[42] *S-K You, Y-W Noh, H-H Park, M. Han, S.S. Lee, S-C Shin, et al.*, "Effect of applying modes of the polymer microneedle-roller on the permeation of L-ascorbic acid in rats", Journal of Drug Targeting, **vol. 18**, issue 1, 2010, pp. 15-20.

[43] *S.A. Burton, C-Y Ng, R. Simmers, C. Moeckly, D. Brandwein, T. Gilbert, et al.*, "Rapid intradermal delivery of liquid formulations using a hollow microstructured array", Pharmaceutical Research. **vol. 28**, issue 1, 2011, pp. 31-40.

[44] *J.S. Kochhar, W.J. Goh, S.Y. Chan, L. Kang*, "A simple method of microneedle array fabrication for transdermal drug delivery", Drug Development and Industrial Pharmacy, **vol. 39**, issue 2, 2013, pp. 299-309.

[45] *J-H. Park, M.G. Allen, M.R. Prausnitz*, "Polymer microneedles for controlled-release drug delivery", Pharmaceutical Research, **vol. 23**, issue 5, 2006, pp. 1008-1019.

[46] *Y. Ito, A. Murakami, T. Maeda, N. Sugioka, K. Takada*, "Evaluation of self-dissolving needles containing low molecular weight heparin (LMWH) in rats", International Journal of Pharmaceutics, **vol. 349**, issue 1, 2008, pp. 124-129.

[47] *G. Li, A. Badkar, S. Nema, C.S. Kolli, A.K. Banga*, "*In vitro* transdermal delivery of therapeutic antibodies using maltose microneedles", International Journal of Pharmaceutics, **vol. 368**, issue 1, 2009, pp. 109-115.

[48] *T. Miyano, T. Miyachi, T. Okanishi, H. Todo, K. Sugibayashi, T. Uemura, et al.*, "Hydrolytic microneedles as Transdermal Drug Delivery System", Solid-State Sensors, Actuators and Microsystems Conference, 2007 TRANSDUCERS 2007 International; 2007: IEEE.

[49] *C. Iliescu C, F.E.H. Tay, J. Wei*, "Low stress PECVD—SiNx layers at high deposition rates using high power and high frequency for MEMS applications", Journal of Micromechanics and Microengineering, **vol.16**, no. 4, 2006, pp. 869-874.

[50] *C. Iliescu, M. Avram, B. Chen, A. Popescu, V. Dumitrescu, D. Poenar et al.*, "Residual stress in thin films PECVD depositions", Journal of Optoelectronics and Advanced Materials, **vol. 13**, issue 4, 2011, pp. 387-394.

[51] *S. Kaushik, A.H. Hord, D.D. Denson, D.V. McAllister, S. Smitra, M.G. Allen et al.*, "Lack of pain associated with microfabricated microneedles", Anesthesia & Analgesia, **vol. 92,** issue 2, 2001, pp. 502-504.

[52] *D. Lipomi, R. Martinez, L. Cademartiri, G. Whitesides*, "Soft Lithographic Approaches to Nanofabrication", Polym Sci Compr Ref. **vol. 10**, 2012, pp. 211-231.